Report

Cell Reports

Long Noncoding RNA Ceruloplasmin Promotes Cancer Growth by Altering Glycolysis

Graphical Abstract

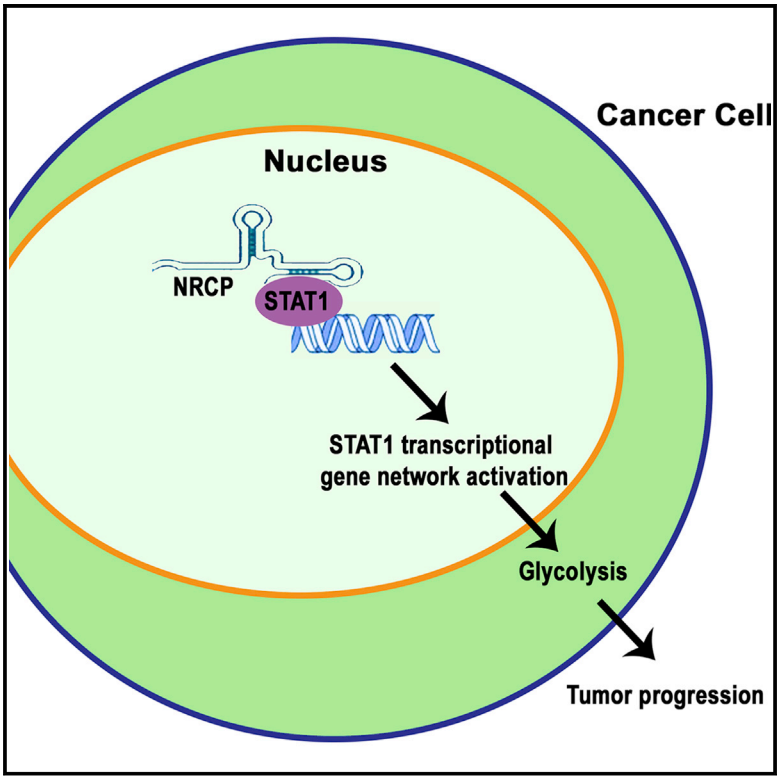

Authors

Rajesha Rupaimoole, Jaehyuk Lee, Monika Haemmerle, ..., Gabriel Lopez-Berestein, Pratip K. Bhattacharya, Anil K. Sood

Correspondence

asood@mdanderson.org

In Brief

The lncRNA NRCP is upregulated in ovarian cancer. Rupaimoole et al. show that NRCP is involved in cancer cell glycolysis and promotes tumor growth and proliferation. They find that silencing NRCP using DOPC-siRNAs in vivo results in robust anti-tumor effects.

Highlights

- Long noncoding RNA NRCP is upregulated in ovarian cancer
- NRCP promotes cancer cell progression by promoting glycolysis
- Silencing NRCP results in apoptosis and decreased tumor progression

Accession Numbers

GSE74447
GSE74448

Rupaimoole et al., 2015, Cell Reports *13*, 2395–2402
December 22, 2015
http://dx.doi.org/10.1016/j.celrep.2015.11.047

Cell Reports
Report

Long Noncoding RNA Ceruloplasmin Promotes Cancer Growth by Altering Glycolysis

Rajesha Rupaimoole,[1,2] Jaehyuk Lee,[3] Monika Haemmerle,[1] Hui Ling,[4] Rebecca A. Previs,[1] Sunila Pradeep,[1] Sherry Y. Wu,[1] Cristina Ivan,[1,5] Manuela Ferracin,[6] Jennifer B. Dennison,[7] Niki M. Zacharias Millward,[3] Archana S. Nagaraja,[1,2] Kshipra M. Gharpure,[1,2] Michael McGuire,[1,2] Nidhin Sam,[1] Guillermo N. Armaiz-Pena,[1] Nouara C. Sadaoui,[1,2] Cristian Rodriguez-Aguayo,[4,5] George A. Calin,[4,5] Ronny I. Drapkin,[8] Jeffery Kovacs,[9] Gordon B. Mills,[7] Wei Zhang,[10] Gabriel Lopez-Berestein,[4,5] Pratip K. Bhattacharya,[3] and Anil K. Sood[1,5,11,*]
[1]Department of Gynecologic Oncology and Reproductive Medicine
[2]Graduate School of Biomedical Sciences
[3]Department of Cancer Systems Imaging
[4]Department of Experimental Therapeutics
[5]Center for RNA Interference and Non-Coding RNAs
The University of Texas MD Anderson Cancer Center, Houston, TX 77030, USA
[6]Department of Experimental and Diagnostic Medicine and Interdepartment Center for Cancer Research, University of Ferrara, Ferrara 44100, Italy
[7]Department of Systems Biology, The University of Texas MD Anderson Cancer Center, Houston, TX 77030, USA
[8]Obstetrics, Gynecology and Pathology, University of Pennsylvania, Philadelphia, PA 19104, USA
[9]Institute of Applied Cancer Science
[10]Department of Pathology
[11]Department of Cancer Biology
The University of Texas MD Anderson Cancer Center, Houston, TX 77030, USA
*Correspondence: asood@mdanderson.org
http://dx.doi.org/10.1016/j.celrep.2015.11.047

SUMMARY

Long noncoding RNAs (lncRNAs) significantly influence the development and regulation of genome expression in cells. Here, we demonstrate the role of lncRNA ceruloplasmin (NRCP) in cancer metabolism and elucidate functional effects leading to increased tumor progression. NRCP was highly upregulated in ovarian tumors, and knockdown of NRCP resulted in significantly increased apoptosis, decreased cell proliferation, and decreased glycolysis compared with control cancer cells. In an orthotopic mouse model of ovarian cancer, siNRCP delivered via a liposomal carrier significantly reduced tumor growth compared with control treatment. We identified NRCP as an intermediate binding partner between STAT1 and RNA polymerase II, leading to increased expression of downstream target genes such as glucose-6-phosphate isomerase. Collectively, we report a previously unrecognized role of the lncRNA NRCP in modulating cancer metabolism. As demonstrated, DOPC nanoparticle-incorporated siRNA-mediated silencing of this lncRNA in vivo provides therapeutic avenue toward modulating lncRNAs in cancer.

INTRODUCTION

Noncoding RNAs (ncRNAs) have been shown to play a significant role in cancer development and progression. These RNAs are divided into multiple families based on their sizes and biogenesis pathways (Mattick and Makunin, 2006; Mercer et al., 2009; Wang and Chang, 2011). Members of one ncRNA family, long ncRNAs (lncRNAs), are genomically transcribed noncoding transcripts longer than 200 nucleotides (Mattick and Makunin, 2006; Mercer et al., 2009). Many lncRNAs are differentially expressed in different tissues and under different developmental and pathological conditions, suggesting that they play important biologic roles (Wang and Chang, 2011; Esteller, 2011; Prensner and Chinnaiyan, 2011; Cheetham et al., 2013). lncRNAs are involved in modulation of cellular functions via regulation of transcription, epigenetic modulation, and enhancement of RNA degradation (Mercer et al., 2009; Wang and Chang, 2011; Prensner and Chinnaiyan, 2011).

Even though several lncRNAs have been discovered using model systems such as yeast, few have been proven to be involved in cancer-specific phenotypes and few are discovered to be involved in cancer metastasis (Gupta et al., 2010; Yuan et al., 2014). Currently, the majority of cancer studies of lncRNAs have focused on a few candidates (Cheetham et al., 2013), such as ANRIL (Yap et al., 2010), lncRNA-ATB (Yuan et al., 2014), PCAT1 (Prensner et al., 2011) in prostate cancer, XIST (Yildirim et al., 2013) in hematologic cancer, MALAT1 in lung cancer (Gutschner et al., 2013), and HOTAIR (Gupta et al., 2010) in breast cancer. These studies have enabled us to understand lncRNA biology in cancers; however, applying this knowledge toward therapeutics is the current need. In the present study, we report upregulation of the lncRNA ceruloplasmin (NRCP) in ovarian cancer and elucidate its functional roles in cancer cells in vitro and in vivo. Intriguingly, we show that NRCP-targeted siRNA using DOPC nanoliposomes significantly reduced tumor

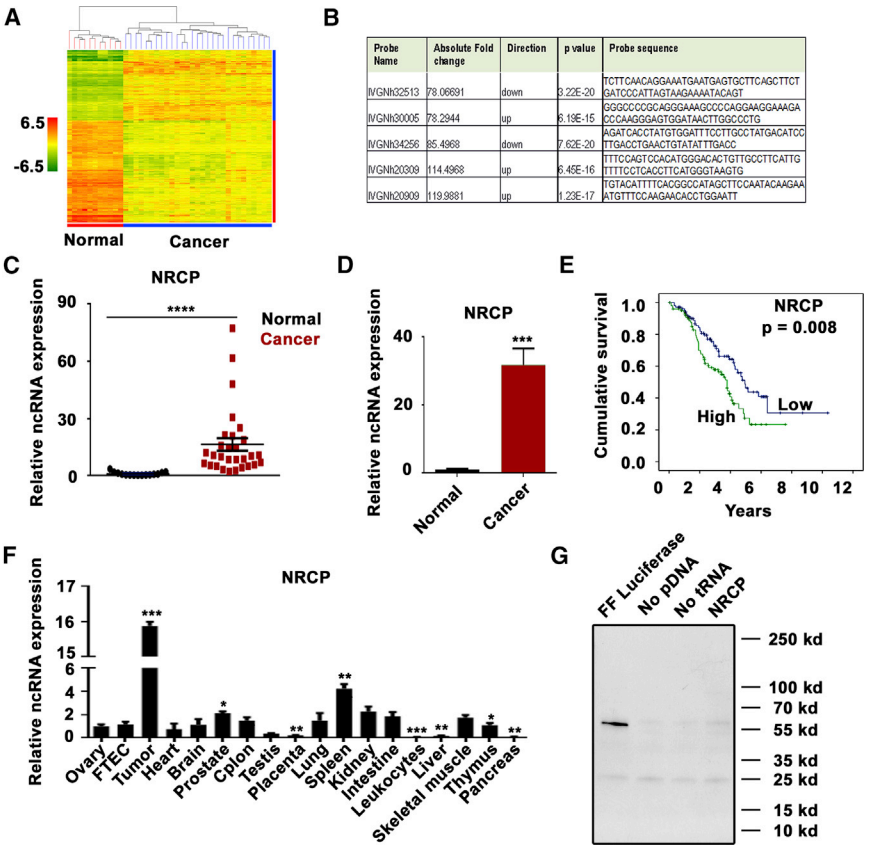

Figure 1. The ncRNA NRCP Is Upregulated in Ovarian Cancer

(A) Heatmap showing the clustering of samples according to expression of ncRNAs.

(B) Table displaying the top five differentially expressed probes, the probe sequences, and p values.

(C) Relative expression of NRCP in ovarian tumor tissues compared with normal ovarian tissue samples, originally used for the ncRNA array.

(D) Relative expression of NRCP in a large cohort (n = 219) of ovarian tumor tissues compared with normal ovarian tissue samples.

(E) Kaplan-Meier overall survival curves for tumor samples analyzed for low and high NRCP expression levels (p = 0.008).

(F) Relative NRCP expression in an array of various normal tissues compared with normal ovary and ovarian tumor samples.

(G) Western blot analysis of samples from in vitro translation assay reactions with NRCP expression plasmid, and also shown are additional lanes of samples from assays with luciferase-positive control plasmid, no plasmid, and no tRNA negative controls.

Data are presented as mean ± SEM of n ≥ 3 experimental groups. *p < 0.05; **p < 0.01; ***p < 0.001; ****p < 0.0001 (Student's t test).

growth and increased sensitivity to cisplatin in orthotopic mouse models of ovarian cancer.

RESULTS

NRCP Deregulation in Ovarian Cancer

Using the human NCode Noncoding RNA Array, we carried out a comparative analysis of lncRNAs in high-grade serous ovarian cancer (n = 29) and normal ovarian (n = 11) samples. We identified >1,000 putative or validated lncRNAs that were deregulated in ovarian cancer tissues compared with normal ovarian tissues (Figure 1A). The top five differentially regulated probes mapped to four lncRNAs (Figure 1B) and were validated in the same clinical samples as those used for the ncRNA array. Two of these lncRNAs were significantly upregulated in ovarian cancer samples compared with normal ovarian tissues (Figures 1C and S1A); levels of the two other lncRNAs differed lesser in magnitude (Figures S1B and S1C). Next, we identified that the NC1 probe corresponds to a lncRNA variant of ceruloplasmin (NRCP). NC2 corresponded to a newly annotated gene that encodes ROGDI homolog protein (Uniprot: Q9GZN7). Genomically, NRCP mapped to chromosome 3 (locus 3q23-q25 of the ceruloplasmin gene). NRCP is a noncoding splice variant of ceruloplasmin-coding gene that lacks exon 11 from the coding region and has several nucleotide changes in the 3′ end exons (Data S1).

We observed significant upregulation of NRCP RNA expression (Figure 1D) and NC2 (Figure S1D) in ovarian tumor samples (n-218) compared with normal ovarian tissues. In Kaplan-Meier survival analyses, patients with low tumoral NRCP expression had significantly better overall survival than those with high NRCP expression (p = 0.008; Figure 1E). However, we observed only a modest survival benefit in patients whose tumors had altered NC2 expression (p = 0.029; Figure S1E). Upon comparing NRCP expression in ovarian tumor samples and in an array of normal tissue samples from various sites in the body, we observed >10-fold higher NRCP expression in the tumor than in normal samples from any site (Figure 1F). In a subset of human ovarian-tumor-derived RNA samples (n = 15), we quantified mRNA expression of ceruloplasmin. Correlation analysis with NRCP expression showed a weak positive correlation (r = 0.29; p = 0.27; Figure S1F). Upon performing in vitro translation assay using NRCP clones in an expression plasmid and rabbit reticulocyte system, we observed no distinct protein bands with the NRCP or negative control reactions (Figure 1G). This further points to the NRCP transcript being noncoding in nature.

NRCP Involvement in Cancer Cell Metabolism

Next, we sought to elucidate the biological functions affected by NRCP to better understand the role of NRCP in ovarian cancer. We selected SKOV3 and A2780 ovarian cancer cells for further studies because of their high NRCP expression (Figure 2A) and in vivo tumorigenicity. To understand whether this lncRNA is expressed in additional cancer cell lines, we measured NRCP expression in breast cancer cell lines. In MDA MB 231 and

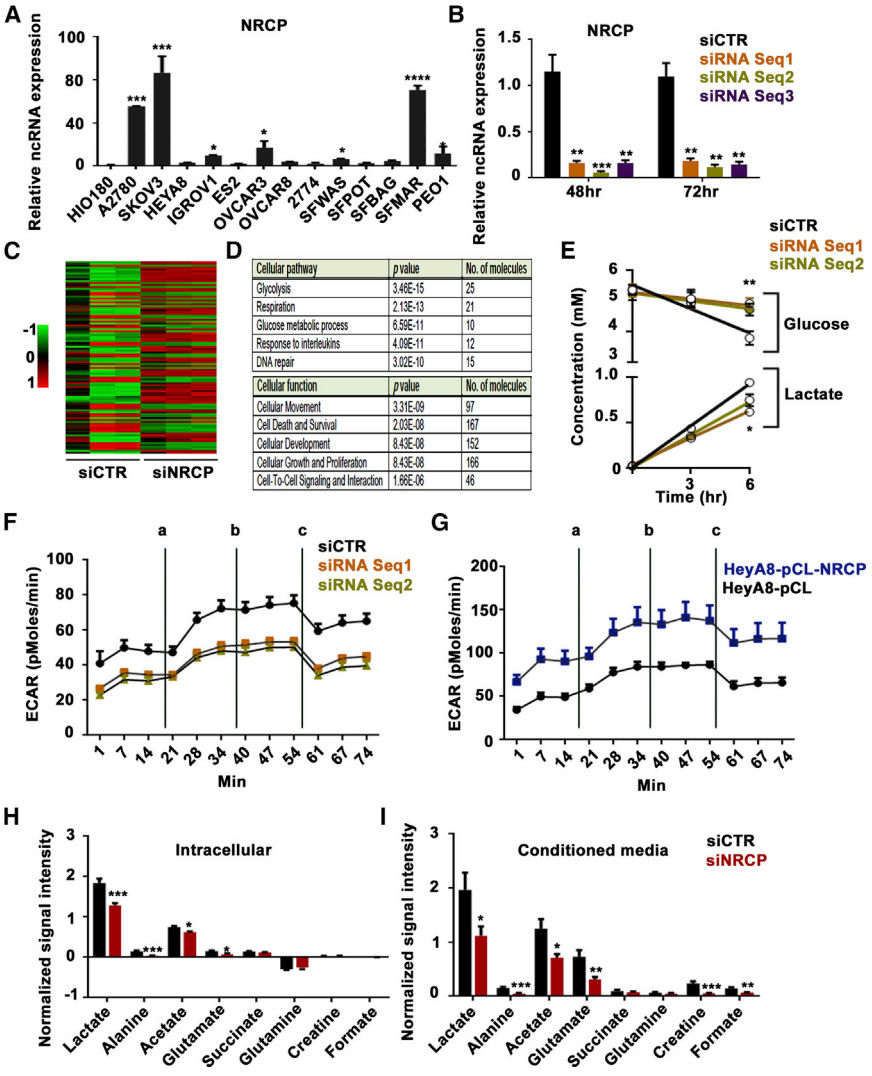

Figure 2. The ncRNA NRCP Is Involved in Regulation of Glycolysis

(A) Relative expression of NRCP in a panel of ovarian cancer cells compared with HIO180 (a transformed ovarian epithelial cell line).

(B) Relative expression of NRCP in SKOV3 cells transfected with siNRCP at different time points.

(C) Heatmap plotted on differentially expressed cDNA probes showing clustering of control siRNA and siNRCP samples. SKOV3 cells and 48 hr of siNRCP were used for the cDNA array.

(D) Table depicting top five altered cellular pathways and cellular function after NRCP knockdown in SKOV3 cells. The array data were analyzed using Ingenuity Pathway Analysis.

(E) Glucose and lactate concentrations in media collected from SKOV3 cells transfected with control siRNA and siNRCP at three different time points (time calculated 48 hr after transfection and addition of fresh media with 5 mM glucose).

(F and G) Glycolysis flux data measured using Seahorse Flux analyzer in SKOV3 cells transfected with siNRCP compared with sicontrol (F), and HeyA8 cells ectopically expressing NRCP compared to control plasmid cells (G). Lines represent addition of (a) glucose, (b) oligomycin, and (c) 2-deoxy-D-glucose.

(H and I) Metabolites levels in control and siNRCP-treated cells. Data from intracellular (H) and conditioned media (I) measured via NMR method are shown.

Data are presented as mean ± SEM of n ≥ 3 experimental groups. *p ≤ 0.05; **p ≤ 0.01; ***p ≤ 0.001; ****p < 0.0001 (Student's t test).

MCF7 cells, we observed significantly increased expression of NRCP, which was comparable to the expression observed in SKOV3 cells (Figure S2A).

Next, we identified two siRNA sequences specific to NRCP (siNRCPs), which reduced its expression by >90% (Figure 2B). We observed no change in the expression of the coding compartment of the ceruloplasmin gene (Figure S2B). From the cDNA array of RNA samples isolated from siNRCP- and sicontrol-treated SKOV3 cells, we observed >2,000 significant gene expression changes ($p < 0.01$) following siNRCP treatment compared with control treatment (Figure 2C). Data were analyzed through the use of QIAGEN's Ingenuity Pathway Analysis (QIAGEN; http://www.ingenuity.com). Top altered cellular pathways were the glycolysis, cellular respiration, and glucose metabolism pathways (Figure 2D, top). The cellular functions most altered by siNRCP were cellular movement, death, and survival functions (Figure 2D, bottom).

After knockdown of NRCP, significant decreases in glucose uptake and decreases in amount of lactate production were observed (Figures 2E and S2C). Parallel with these data, significant decreases in glycolytic flux (ECAR) were observed in SKOV3 and A2780 cells treated with siNRCP compared to control cells (Figures 2F and S2D). Conversely, upon overexpression of NRCP, HeyA8 cells showed significant increase in ECAR (Figure 2G), indicative of increased glycolysis in these cells. There was significant increase in basal respiration and ATP-synthase-dependent respiration in siNRCP—compared to control-treated cells (Figure S2E). Measurement of metabolites in cancer cells (intracellular) and conditioned media after silencing NRCP showed a significant reduction in several metabolites compared to controls (Figures 2H and 2I). Among the metabolites changed, lactate showed the greatest decrease (>40%; Figures 2H and 2I). This further confirmed the reduction of glycolysis-mediated metabolites because pyruvate acts as an important intermediate for TCA cycle progression.

Biological Functions Involving NRCP in Ovarian Cancer

Our observations from microarray data analysis showed that cell death, survival, growth, and proliferation are the main cellular functions affected by NRCP silencing (Figure 2D). To understand this potential link between reversal of metabolism, reduced tumor growth, and NRCP, we carried out cellular functional assays after silencing NRCP in SKOV3 and A2780 ovarian cancer cells.

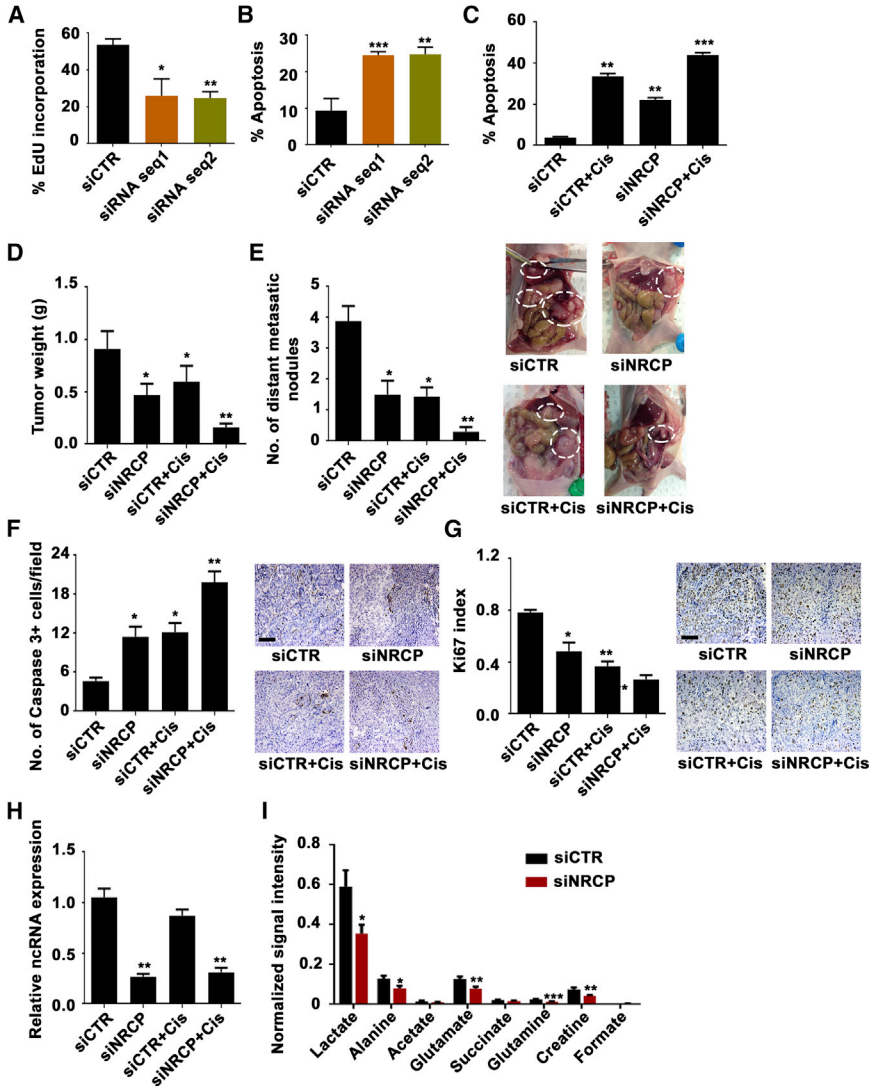

Figure 3. Silencing NRCP Decreases Cancer Cell Growth and Metastasis

(A and B) Proliferation measured as percentage of EdU incorporation (A) and apoptosis measured via annexin V staining (B) in control siRNA- and siNRCP-treated SKOV3 cells measured 72 hr after transfection.

(C) Percentages of apoptotic cells in control siRNA- and siNRCP-treated SKOV3 cells with or without an IC_{50} dose of cisplatin.

(D) Effect of in vivo silencing of NRCP in an SKOV3 orthotopic model of ovarian cancer. Aggregate tumor weights are shown in mice treated with control siRNA, siNRCP, and combinations with cisplatin (n = 10 per group).

(E) Average numbers of distant metastatic nodules across the four groups. Representative pictures of tumor burden in each treatment group are shown in side panel.

(F and G) Immunohistochemistry data illustrating apoptosis via caspase 3+ staining (F) and proliferation via the Ki67 index (G) across the four groups of tumors harvested.

(H) Relative expression of NRCP in tumors harvested from individual groups of mice treated with control siRNA, siNRCP, and combinations with cisplatin.

(I) Levels of metabolite in tumor tissue samples treated with control siRNA or siNRCP; data were obtained via NMR method.

Data are presented as mean ± SEM of n ≥ 3 experimental groups. *p < 0.05; **p < 0.01; ***p < 0.001 (Student's t test).

There was a significant reduction in 5-ethynyl-2′-deoxyuridine (EdU) incorporation in SKOV3 and A2780 cells transfected with siNRCP compared with sicontrol-treated cells (see Figure 3A for SKOV3 and Figure S3A for A2780). Annexin V staining showed significantly more apoptosis in siNRCP-treated SKOV3 cells than in sicontrol-treated cells (see Figure 3B for SKOV3 and Figure S3B for A2780). Cell-cycle analysis of SKOV3 cells treated with siNRCP revealed a significant reduction of cells in the S phase and accumulation of cells at G2 compared with control-treated cells, suggesting an increase in cellular apoptosis following G2 arrest (Figure S3C). Cells treated with siNRCP showed significant reduction in cyclin B1, suggesting G2 cell-cycle arrest, whereas CDK1 showed no such change (Figure S3D). Consistent with the above data, we observed a significant reduction in cell viability in siNRCP-treated SKOV3 cells compared with sicontrol-treated cells (Figure S3E).

Because silencing NRCP significantly reduced cell viability, we next asked whether siNRCP would be even more effective in combination with commonly used chemotherapeutic agents for ovarian cancer treatment. We observed a significant shift in sensitivity of SKOV3 cells to cisplatin after NRCP gene knockdown (Figure S3F); however, we did not see sensitization to docetaxel with NRCP knockdown (Figure S3F). To validate this observation, we treated SKOV3 cells with siNRCP, cisplatin, or siNRCP plus cisplatin and performed an annexin V apoptosis assay. Apoptosis was increased in the cells treated with siNRCP combined with cisplatin than in those treated with sicontrol, siNRCP alone, or cisplatin alone (Figures 3C and S3G). Conversely, we observed decreased cell apoptosis and increased cell proliferation in cells ectopically expressing NRCP compared to control cells (Figure S3H).

Considering that cellular movement pathways were also affected by NRCP gene knockdown (Figure 2D), we assessed the migration and invasion potential of SKOV3 cells treated with siNRCP. Consistent with the findings from the microarray analyses, knockdown of NRCP significantly reduced migration and invasion of SKOV3 cells (Figure S3J).

In Vivo Effects of NRCP Silencing in Ovarian Cancer Models

Next, we evaluated the effects of NRCP silencing on tumor growth and metastasis in vivo in a murine orthotopic model of

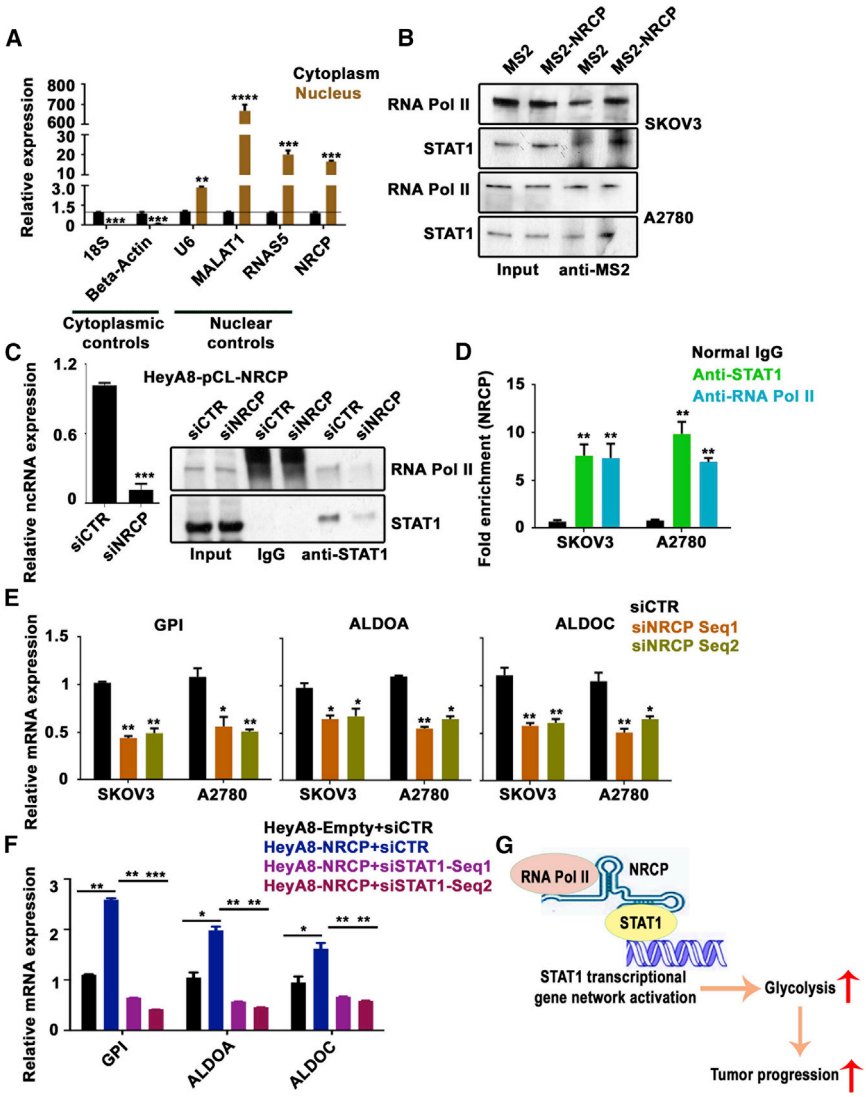

Figure 4. NRCP Regulates Cancer Cell Glycolysis by Binding to STAT1

(A) Relative expression of NRCP, cytoplasmic control RNAs 18S and β-actin and nuclear control RNAs U6, MALAT1, and 5.8S rRNA in RNA samples isolated from nuclear and cytoplasmic cell fractionations of SKOV3 cells.

(B) Western blot data from GSH-agarose immunoprecipitation of protein lysates from SKOV3 cells transfected with pMS2-control and pMS2-NRCP plasmid. Membranes were probed for RNA pol II and STAT1 using corresponding antibodies.

(C) Data show expression of NRCP in HeyA8-pCL-NRCP cells transfected with siRNA against NRCP (right). Western blot data show binding of RNA pol II and STAT1 (left). HeyA8-pCL-NRCP cells were treated with sicontrol and siNRCP; cell lysates were subjected to immunoprecipitation using an anti-STAT1 antibody.

(D) RIP assay qPCR data showing significant fold enrichment in NRCP binding to STAT1 and RNA pol II. Data normalized to IgG isotype control immunoprecipitation.

(E and F) RNA expression of key glycolysis pathway proteins GPI, ALDOA, and ALDOC in cells transfected with siRNA against NRCP (E) or HeyA8 cells ectopically expressing NRCP, with and without siNRCP transfected (F), compared to respective sicontrols.

(G) Summary of study showing mechanism by which NRCP mediates increased glycolysis in cancer.

Data are presented as mean ± SEM of n ≥ 3 experimental groups. *p < 0.05; **p < 0.01; ***p < 0.001 (Student's t test).

ovarian cancer using intra-ovarian injection of SKOV3 cells. There was significant reduction in gross tumor weight in the DOPC-siNRCP-treated mice compared to DOPC-sicontrol-treated group (Figure 3D). In addition, compared to the mice treated with sicontrol, mice treated with siNRCP and cisplatin combination showed significant tumor reduction and metastasis (Figures 3D and 3E). Immunohistochemistry staining for cleaved caspase-3 in tumor tissues from all four groups showed significantly increased apoptosis in the groups treated with siNRCP, cisplatin, or siNRCP plus cisplatin compared with the control group (Figure 3F). In addition, quantitation of proliferation via the Ki67 index showed significant reductions in cell proliferation in the groups treated with siNRCP, cisplatin, or siNRCP plus cisplatin compared with the sicontrol group (Figure 3G). NRCP expression in the tumors from siNRCP groups was reduced by >75% compared to tumors from sicontrol group (Figure 3H). Metabolite analyses from these samples revealed significant reduction in lactate levels in the tumors treated with siNRCP compared to sicontrol (Figure 3I), further supporting the in vitro observations. We also evaluated the in vivo effects of NRCP silencing using the ovarian cancer cell line A2780. We observed tumor size reduction and fewer metastatic nodules in A2780 tumor-bearing mice treated with siNRCP, cisplatin, or siNRCP plus cisplatin compared with the control group (Figures S3K–S3N), as observed in the in vivo NRCP-silencing study with SKOV3 cells.

Mechanisms Underlying the NRCP-Glycolysis Link in Cancer Cells

Using nuclear and cytoplasmic fractionation from cell lysates and quantification of RNA abundance using qRT-PCR, we observed significant enrichment of NRCP in the nucleus compared to the cytoplasmic fraction in SKOV3, A2780, and HeyA8 cells with ectopic expression of NRCP (Figures 4A, S4A, and S4B). Using the bait system (Yoon et al., 2012) of MS2 protein-MS2 RNA affinity interactions and mass spectrometry analysis, we identified ~190 unique proteins binding to NRCP. From the analysis of their localization, cellular functions, and potential involvement in glycolysis pathways, we identified STAT1 as a key candidate potentially binding to NRCP

(Table S1; Figure S4C). The role of STAT1 in modulating cancer cell metabolism was suggested earlier (Pitroda et al., 2009); however, mechanisms were not identified. Immunoprecipitation using GSH-conjugated agarose beads and western blotting revealed significant binding of NRCP to STAT1 (Figure 4B). Because STAT1 transcription programming involves binding of RNA pol II, we checked whether NRCP facilitates the interactions between STAT1 and RNA pol II. Upon probing the western blot described above with anti-RNA pol II, we observed significant binding of RNA pol II to MS2-NRCP (Figure 4B). Next, we ectopically expressed NRCP in HeyA8 cells and used siRNAs against NRCP to decrease the expression, followed by immunoprecipitation with anti-STAT1. In the sicontrol-treated HeyA8-NRCP cells, upon anti-STAT1 pull-down and western blotting for RNA pol II, we identified clear binding of STAT1 with RNA pol II (Figure 4C). Interestingly, we observed significant decrease in RNA pol II binding to STAT1 upon silencing NRCP (Figure 4C), suggesting the role of NRCP as an intermediate molecule facilitating STAT1-RNA pol II interactions. In a different approach, we performed RNA-immunoprecipitation (RIP) assay using anti-STAT1 and anti-RNA pol II antibodies in SKOV3 cells. NRCP showed significant enrichment in binding to STAT1 and RNA pol II in RIP RNA samples (Figure 4D), further supporting the link between NRCP and these two proteins. We used MALAT1 and U1 as controls for RIP reactions (Figures 4D and 4E). After silencing or rescuing NRCP in cancer cells, we tested expression of key glycolysis pathway molecules suggested from the genomic array of siNRCP-treated SKOV3 cells (Ingenuity Pathway Analysis; Data S2). Significant reduction in glucose-6-phosphate isomerase (GPI), ALDOA, and ALDOC was observed after silencing NRCP in SKOV3 or A2780 cells (Figure 4E). Conversely, upon rescue of NRCP expression in HeyA8 cells, we observed significant increase in the expression of these molecules compared to control cells (Figure 4F). Upon silencing STAT1 in the cells ectopically expressing NRCP, we observed significant reduction in the expression of GPI, ALDOA, and ALDOC (Figure 4F), further strengthening the role played by NRCP-STAT1 axis in regulating glycolysis. In summary, our data show that NRCP is involved in glycolysis regulation in cancer cells through NRCP acting as an intermediate molecule between STAT1 and RNA pol II, enhancing their interactions, leading to increased STAT1 transcriptional programming (Figure 4G).

DISCUSSION

In this study, we elucidated the role of the lncRNA NRCP in metabolic alterations in cancer cells. By profiling ncRNA expression in human normal ovaries and ovarian tumors, we identified NRCP as the top-upregulated lncRNA in ovarian cancer. We report that silencing NRCP significantly decreases glycolysis and increases mitochondrial respiration in cancer cells. This ultimately led to enhanced cancer cell apoptosis and decreased cell proliferation. Using orthotopic ovarian cancer mouse models, we further demonstrated the profound reduction in primary tumor growth and cancer metastasis following delivery of nanoliposome-delivered siNRCP to tumors.

Studies have shown that cancer cells rely on glycolysis for energy production, whereas normal cells rely on the oxidative pathway (Warburg, 1956; Vander Heiden et al., 2009). Inhibition of lactate production is suggested to have significant therapeutic benefits in cancer (Doherty and Cleveland, 2013). In a recent lung cancer study, reversal of Warburg effect by inhibition of EGFR signaling resulted in significant tumor reduction (De Rosa et al., 2015) and highlights the potential for the therapeutic targeting of glycolysis. Currently, there is limited data on role of lncRNAs in regulating cancer metabolism. Whereas Li et al. (2014) have recently reported the role of the lncRNA UCA1 in hexokinase dysfunction, this study was limited to in vitro observations. A lncRNA specific to prostate cancer called PCGEM1 was shown to be involved in promoting cancer cell metabolism mediated by binding of this lncRNA to MYC transcription factor and activation of downstream genes (Hung et al., 2014). These suggest evolving roles of lncRNAs in cancer cell metabolism and show great promise toward use of this knowledge for therapeutic applications.

The use of siRNA-based approaches for silencing these chemically non-targetable genes is suggested by several studies. One of the recent developments in the delivery of siRNA is the liposomal carrier DOPC, which enables efficient delivery of siRNA molecules to the tumor microenvironment (Nishimura et al., 2013; Wu et al., 2014). Preclinical studies by our group have shown targeting EphA2 in ovarian cancer (Kamat et al., 2009) using the same approach, which is currently entering clinical trials (NCT01591356). In the present study, we used a similar approach to target a lncRNA in vivo using a siRNA against NRCP incorporated in a DOPC liposomal carrier.

In summary, our findings reveal a novel role of lncRNAs in cancer metabolism. Our study provides a basis for further development and application of RNAi-based therapeutic approaches to target lncRNAs and shows an expanded potential for siRNA-based therapeutics for more-effective treatment of diseases such as cancer.

EXPERIMENTAL PROCEDURES

Cell Line Maintenance and siRNA Transfections

All the cell lines used were obtained from the ATCC and were maintained in RPMI1640 medium supplemented with 10%–15% fetal bovine serum and 0.1% gentamicin sulfate (Gemini Bio-Products) in 5% CO_2 at 37°C. All cell lines were routinely tested to confirm the absence of Mycoplasma, and all in vitro experiments were conducted with 60%–80% confluent cultures. For detailed procedure, please refer to Supplemental Experimental Procedures.

In Vivo Models

Female athymic nude mice were purchased from Taconic Farms. These animals were cared for according to guidelines set forth by the American Association for Accreditation of Laboratory Animal Care and the United States Public Health Service policy on Humane Care and Use of Laboratory Animals. All mouse studies were approved and supervised by The University of Texas MD Anderson Cancer Center Institutional Animal Care and Use Committee. All mice used were 8–12 weeks old at the time of treatment. The orthotopic mouse models of ovarian cancer were developed as described previously (Pecot et al., 2013; Pradeep et al., 2014). For all experiments, mice were randomly divided and treated with intraperitoneal administration of siRNA incorporated in neutral DOPC nanoliposomes prepared as previously described (Kamat et al., 2009; Nishimura et al., 2013; Pecot et al., 2013; Pradeep et al., 2014). For detailed procedure, please refer to the Supplemental Experimental Procedures.

Identification of NRCP-Binding Proteins

To identify potential protein-binding partners of NRCP, we used the MS2-tagged RNA affinity purification technique (Yoon et al., 2012). Briefly, we

cloned full-length NRCP into pMS2 plasmid containing MS2 repeats. SKOV3 cells were transfected with pMS2 plasmids (control or NRCP) and MS2-GST plasmids (a fusion protein recognizing the MS2 RNA hairpins), and cell lysates were prepared according to previously described protocol (Yoon et al., 2012). MS2 protein-MS2 RNA-NRCP complex along with associated proteins were immunoprecipitated using GSH-conjugated agarose beads. We eluted protein complex from agarose beads and subjected the samples to mass spectrometry analysis at MD Anderson Cancer Center Proteomics core facility. Identified proteins from MS/MS analysis were compared between pMS2-control and pMS2-NRCP to identified NRCP-bound proteins. Using Ingenuity Pathway Analysis, we characterized these proteins according to their cellular localization and functions to identify top candidates to confirm the interactions with NRCP.

Microarrays and Data Analysis

Total RNA was extracted from the ovarian tumor samples and normal ovarian tissues using the mirVana RNA Isolation kit (Life Technologies). Expression levels of ncRNAs were profiled using NCode Noncoding RNA Array (Invitrogen). Microarray results were analyzed by using GeneSpring GX software, version 12.6 (Agilent Technologies). For detailed procedure, please refer to Supplemental Experimental Procedures.

Immunostaining, Cell Proliferation, Cell Viability, Cell Cycle, and Apoptosis Assays

For immunohistochemical analyses, 5-μm paraffin sections of tumor tissues were used for the detection of the proliferation marker Ki67 and the apoptosis marker cleaved caspase-3. For Ki67 and cleaved caspase-3 staining, the numbers of tumor cells that were positive for expression were counted. Modified Boyden chambers (Coster) coated with 0.1% gelatin or extracellular matrix components were used to measure migration and invasion, respectively. Post assay, cells were fixed and stained, and then cells from five random fields were counted using light microscopy. For detailed procedure, please refer to Supplemental Experimental Procedures.

In Vitro Translation Assay

NRCP-pCL-Neo with full-length NRCP and luciferase-positive control plasmid was used for in vitro translation assays using the TnT Quick Coupled Transcription/Translation System (Promega) with 1 mM methionine and Transcend Biotin-Lysyl-tRNA (Promega) according to the manufacturer's instructions. For detailed procedure, please refer to Supplemental Experimental Procedures.

Measurement of Glycolysis and Respiration Rate

The Seahorse Extracellular Flux Analyzer XF96 (Seahorse Bioscience) was used to measure oxygen consumption rate upon silencing NRCP using siRNAs. For glycolysis measurements, we added glucose, oligomycin, and deoxy-glucose to measure basal flux rates glycolytic capacity and to inhibit glycolysis, respectively. For detailed procedure, please refer to the Supplemental Experimental Procedures.

RIP Assays

RIP assays were performed using a Millipore EZ-Magna RIP RNA-Binding Protein Immunoprecipitation kit (Millipore; 17-701) according to the manufacturer's instructions. For detailed procedure, please refer to the Supplemental Experimental Procedures.

NMR Measurement of Metabolites

For the measurement of metabolite in media studies, we collected conditioned media from cells treated with sicontrol and siNRCP for 48 hr. Cell pellets or tumor tissue samples were used for measurement of intracellular metabolite levels. Analyses of samples were done using nuclear magnetic resonance (NMR) spectroscopy. For in vitro measurements, cell counts were used to normalize the data. For in vivo tumor samples, data normalized to tissue weight and intratumor level of NRCP measured by qPCR. For detailed procedure, please refer to the Supplemental Experimental Procedures.

ACCESSION NUMBERS

The accession numbers for the data reported in this paper are GEO: GSE74447 and GEO: GSE74448.

SUPPLEMENTAL INFORMATION

Supplemental Information includes Supplemental Experimental Procedures, four figures, one table, and two data files and can be found with this article online at http://dx.doi.org/10.1016/j.celrep.2015.11.047.

AUTHOR CONTRIBUTIONS

R.R. and A.K.S. conceived the project and designed the experiments. R.R., R.A.P., S.P., J.L., S.Y.W., A.S.N., K.M.G., M.M., N.M.Z.M., N.S., G.N.A.-P., N.C.S., H.L., and M.H. carried out or participated in in vitro and in vivo experiments. C.R.-A. and G.L.-B. designed and prepared liposomes for in vivo studies. R.I.D. provided fallopian tube epithelial cell samples. R.R., M.F., and C.I. designed and performed computational analyses. R.R. and A.K.S. participated in obtaining and analyzing the clinical data. R.R. wrote the manuscript. J.L., N.M.Z.M., P.K.B., J.B.D., G.B.M., and J.K. helped with measurement of metabolites and performing seahorse flux analysis. W.Z. provided help with the ncRNA array analysis. R.R., R.A.P., G.A.C., and A.K.S. participated in manuscript preparation. All authors edited and approved the final manuscript.

ACKNOWLEDGMENTS

We thank the following for funding support. Portions of this work were supported by the NIH (P30 CA016672, CA109298, UH3TR000943, P50 CA083639, P50 CA098258, U54 CA151668, and U24CA143835), the CPRIT (RP110595), the Ovarian Cancer Research Fund, the United States DOD (OC073399, W81XWH-10-1-0158, and BC085265), the Marcus Foundation, the Red and Charline McCombs Institute for the Early Detection and Treatment of Cancer, the RGK Foundation, the Gilder Foundation, the Blanton-Davis Ovarian Cancer Research Program, and the Betty Anne Asche Murray Distinguished Professorship (to A.K.S.). R.R. is supported in part by the Russell and Diana Hawkins Family Foundation Discovery Fellowship. S.Y.W. is supported by the Ovarian Cancer Research Fund, Foundation for Women's Cancer, and Cancer Prevention and Research Institute of Texas training grants (RP101502 and RP101489). M.H. is supported by the Deutsche Forschungsgemeinschaft (DFG).

Received: September 28, 2015
Revised: November 4, 2015
Accepted: November 15, 2015
Published: December 10, 2015

REFERENCES

Cheetham, S.W., Gruhl, F., Mattick, J.S., and Dinger, M.E. (2013). Long noncoding RNAs and the genetics of cancer. Br. J. Cancer *108*, 2419–2425.

De Rosa, V., Iommelli, F., Monti, M., Fonti, R., Votta, G., Stoppelli, M.P., and Del Vecchio, S. (2015). Reversal of Warburg Effect and Reactivation of Oxidative Phosphorylation by Differential Inhibition of EGFR Signaling Pathways in Non-Small Cell Lung Cancer. Clin. Cancer Res. *21*, 5110–5120.

Doherty, J.R., and Cleveland, J.L. (2013). Targeting lactate metabolism for cancer therapeutics. J. Clin. Invest. *123*, 3685–3692.

Esteller, M. (2011). Non-coding RNAs in human disease. Nat. Rev. Genet. *12*, 861–874.

Gupta, R.A., Shah, N., Wang, K.C., Kim, J., Horlings, H.M., Wong, D.J., Tsai, M.C., Hung, T., Argani, P., Rinn, J.L., et al. (2010). Long non-coding RNA HOTAIR reprograms chromatin state to promote cancer metastasis. Nature *464*, 1071–1076.

Gutschner, T., Hämmerle, M., Eissmann, M., Hsu, J., Kim, Y., Hung, G., Revenko, A., Arun, G., Stentrup, M., Gross, M., et al. (2013). The noncoding

RNA MALAT1 is a critical regulator of the metastasis phenotype of lung cancer cells. Cancer Res. *73*, 1180–1189.

Hung, C.L., Wang, L.Y., Yu, Y.L., Chen, H.W., Srivastava, S., Petrovics, G., and Kung, H.J. (2014). A long noncoding RNA connects c-Myc to tumor metabolism. Proc. Natl. Acad. Sci. USA *111*, 18697–18702.

Kamat, A.A., Coffey, D., Merritt, W.M., Nugent, E., Urbauer, D., Lin, Y.G., Edwards, C., Broaddus, R., Coleman, R.L., and Sood, A.K. (2009). EphA2 overexpression is associated with lack of hormone receptor expression and poor outcome in endometrial cancer. Cancer *115*, 2684–2692.

Li, Z., Li, X., Wu, S., Xue, M., and Chen, W. (2014). Long non-coding RNA UCA1 promotes glycolysis by upregulating hexokinase 2 through the mTOR-STAT3/microRNA143 pathway. Cancer Sci. *105*, 951–955.

Mattick, J.S., and Makunin, I.V. (2006). Non-coding RNA. Hum. Mol. Genet. *15*, R17–R29.

Mercer, T.R., Dinger, M.E., and Mattick, J.S. (2009). Long non-coding RNAs: insights into functions. Nat. Rev. Genet. *10*, 155–159.

Nishimura, M., Jung, E.J., Shah, M.Y., Lu, C., Spizzo, R., Shimizu, M., Han, H.D., Ivan, C., Rossi, S., Zhang, X., et al. (2013). Therapeutic synergy between microRNA and siRNA in ovarian cancer treatment. Cancer Discov. *3*, 1302–1315.

Pecot, C.V., Rupaimoole, R., Yang, D., Akbani, R., Ivan, C., Lu, C., Wu, S., Han, H.D., Shah, M.Y., Rodriguez-Aguayo, C., et al. (2013). Tumour angiogenesis regulation by the miR-200 family. Nat. Commun. *4*, 2427.

Pitroda, S.P., Wakim, B.T., Sood, R.F., Beveridge, M.G., Beckett, M.A., MacDermed, D.M., Weichselbaum, R.R., and Khodarev, N.N. (2009). STAT1-dependent expression of energy metabolic pathways links tumour growth and radioresistance to the Warburg effect. BMC Med. *7*, 68.

Pradeep, S., Kim, S.W., Wu, S.Y., Nishimura, M., Chaluvally-Raghavan, P., Miyake, T., Pecot, C.V., Kim, S.J., Choi, H.J., Bischoff, F.Z., et al. (2014). Hematogenous metastasis of ovarian cancer: rethinking mode of spread. Cancer Cell *26*, 77–91.

Prensner, J.R., and Chinnaiyan, A.M. (2011). The emergence of lncRNAs in cancer biology. Cancer Discov. *1*, 391–407.

Prensner, J.R., Iyer, M.K., Balbin, O.A., Dhanasekaran, S.M., Cao, Q., Brenner, J.C., Laxman, B., Asangani, I.A., Grasso, C.S., Kominsky, H.D., et al. (2011). Transcriptome sequencing across a prostate cancer cohort identifies PCAT-1, an unannotated lincRNA implicated in disease progression. Nat. Biotechnol. *29*, 742–749.

Vander Heiden, M.G., Cantley, L.C., and Thompson, C.B. (2009). Understanding the Warburg effect: the metabolic requirements of cell proliferation. Science *324*, 1029–1033.

Wang, K.C., and Chang, H.Y. (2011). Molecular mechanisms of long noncoding RNAs. Mol. Cell *43*, 904–914.

Warburg, O. (1956). On the origin of cancer cells. Science *123*, 309–314.

Wu, S.Y., Lopez-Berestein, G., Calin, G.A., and Sood, A.K. (2014). RNAi therapies: drugging the undruggable. Sci. Transl. Med. *6*, 240ps7.

Yap, K.L., Li, S., Muñoz-Cabello, A.M., Raguz, S., Zeng, L., Mujtaba, S., Gil, J., Walsh, M.J., and Zhou, M.M. (2010). Molecular interplay of the noncoding RNA ANRIL and methylated histone H3 lysine 27 by polycomb CBX7 in transcriptional silencing of INK4a. Mol. Cell *38*, 662–674.

Yildirim, E., Kirby, J.E., Brown, D.E., Mercier, F.E., Sadreyev, R.I., Scadden, D.T., and Lee, J.T. (2013). Xist RNA is a potent suppressor of hematologic cancer in mice. Cell *152*, 727–742.

Yoon, J.H., Srikantan, S., and Gorospe, M. (2012). MS2-TRAP (MS2-tagged RNA affinity purification): tagging RNA to identify associated miRNAs. Methods *58*, 81–87.

Yuan, J.H., Yang, F., Wang, F., Ma, J.Z., Guo, Y.J., Tao, Q.F., Liu, F., Pan, W., Wang, T.T., Zhou, C.C., et al. (2014). A long noncoding RNA activated by TGF-β promotes the invasion-metastasis cascade in hepatocellular carcinoma. Cancer Cell *25*, 666–681.